Mon. Not. R. Astron. Soc. **000**, 1–7 (0000) Printed 11 December 2008 (MN LATEX style file v2.2)

The nonlinear probability distribution function in models with local primordial non-Gaussianity

Tsz Yan Lam⋆ & Ravi K. Sheth⋆
Department of Physics & Astronomy, University of Pennsylvania, 209 S. 33rd Street, Philadelphia, PA 19104, USA

11 December 2008

ABSTRACT
We use the spherical evolution approximation to investigate nonlinear evolution from the non-Gaussian initial conditions characteristic of the local f_{nl} model. We provide an analytic formula for the nonlinearly evolved probability distribution function of the dark matter which shows that the underdense tail of the nonlinear PDF in the f_{nl} model should differ significantly from that for Gaussian initial conditions. Measurements of the underdense tail in numerical simulations may be affected by discreteness effects, and we use a Poisson counting model to describe this effect. Once this has been accounted for, our model is in good quantitative agreement with the simulations.

Key words: methods: analytical - dark matter - large scale structure of the universe

1 INTRODUCTION

The most common inflation model (the single scalar field, slow-roll inflation) predicts the primordial perturbations to be approximately described by the Gaussian statistics. Detections of non-gaussianity can discriminate between different inflation models, so the study of various cosmological probes of primordial non-gaussianity has attracted much recent attention.

For example, the CMB has been used to constrain non-gaussianity (Komatsu et al. 2008; Hikage et al. 2008; Yadav & Wandelt 2008; McEwen et al. 2008). In addition, various aspects of large scale structure have also been examined as probes of non-gaussianity. These include halo abundances and bias (Lucchin et al. 1988; Robinson & Baker 2000; Matarrese et al. 2000; Lo Verde et al. 2008; Dalal et al. 2008; Matarrese & Verde 2008; Carbone et al. 2008; Afshordi & Tolley 2008; Slosar et al. 2008; Desjacques et al. 2008); higher order effects on the galaxy power spectrum (McDonald 2008; Taruya et al. 2008); and the galaxy bispectrum (Scoccimarro et al. 2004; Sefusatti & Komatsu 2007). And, Slosar (2008) has discussed how to optimize the constraint on f_{nl} by applying weightings on subsamples from a single tracer.

Recently, Grossi et al. (2008) used N-body simulations to study the effect of primordial non-gaussianity on the nonlinear probability distribution function (PDF) of the dark matter field. They found that departures from the Gaussian prediction are strongest in underdense regions and on small scales. The main goal of the present study is to provide some analytic understanding of their results. We do this by studying the nonlinear evolution of the dark matter PDF. When the initial conditions are Gaussian, then the nonlinear evolution can be modelled by the spherical and ellipsoidal collapse models (Lam & Sheth 2008a,b). In these models, the evolution of the PDF depends on two ingredients: a model for the dynamical evolution from an initial state to a final one, and the appropriate average over the initial states. In particular, the spherical and ellipsoidal collapse models approximate the nonlinear dynamics as 1→1 or 3→1 mappings from the initial to the final state that do not depend on the Gaussianity of the initial conditions. Primordial non-Gaussianity enters only because it determines the initial set of states. As a result, essentially all of the machinery developed for the Gaussian case can be simply carried over to the present study.

We recap the definitions of the local non-gaussian f_{nl} model in Section 2.1. The effect of smoothing the initial distribution is described in Section 2.2. Section 2.3 describes the nonlinear PDF associated with the spherical evolution model and compares the results with the Gaussian case. Section 2.4 compares our predictions with measurements in simulations. We summarise our results in Section 3.

⋆ E-mail: tylam@sas.upenn.edu, shethrk@physics.upenn.edu

2 THE PDF OF THE DENSITY IN THE LOCAL NON-GAUSSIAN MODEL

In the f_{nl} models of current interest, the initial density fluctuation field is only mildly perturbed from the Gaussian. Therefore, following Lo Verde et al. (2008) and Desjacques et al. (2008), we use the Edgeworth expansion as a convenient way to summarize our results. Because we are interested in mass scales which are substantially larger than that of a single collapsed halo – the regimes studied by Lo Verde et al. (2008) and Desjacques et al. (2008) – we are certainly in the regime where the Edgeworth expansion is a useful approximation.

2.1 The unsmoothed initial distribution

The primordial perturbation potential Φ of the local non-gaussian field is

$$\Phi = \phi + f_{nl}(\phi^2 - \langle\phi^2\rangle), \tag{1}$$

where ϕ is a Gaussian potential field and f_{nl} is a scalar. We will use $P_\phi(k)$ to represent the power spectrum of ϕ; in what follows we will set $P_\phi(k) = Ak^{n_s-4}$, where $n_s \approx 1$, and A is a normalization constant that is fixed by requiring that the rms fluctuations in the associated non-Gaussian initial density field (which we will define shortly) have value σ_8.

We define $\boldsymbol{M}$ as the real, symmetric 3×3 tensor whose components are proportional to the second order derivatives of the potential Φ:

$$\Phi_{ij} \equiv \phi_{ij} + 2f_{nl}(\phi_i\phi_j + \phi\phi_{ij}), \tag{2}$$

where $\phi_i = \partial_i\phi$ and $\phi_{ij} = \partial_i\partial_j\phi$. We will sometimes refer to $\boldsymbol{M}$ as the shear or deformation tensor associated with the potential Φ.

Correlations between the Φ_{ij} will be very useful in what follows. These depend on the correlations between ϕ and its derivatives. However, because ϕ is Gaussian, they can be computed easily. Specifically,

$$\langle\phi\phi\rangle = \sigma_0^2 \qquad \langle\phi_i\phi\rangle = 0, \qquad \langle\phi_i\phi_j\rangle = \frac{\sigma_1^2}{3}\delta_{ij} \tag{3}$$

$$\langle\phi_{ij}\phi\rangle = -\frac{\sigma_1^2}{3}\delta_{ij} \qquad \langle\phi_{ij}\phi_k\rangle = 0, \qquad \langle\phi_{ij}\phi_{kl}\rangle = \frac{\sigma_2^2}{15}\delta_{ijkl} \tag{4}$$

where δ_{ij} is the dirac delta function, and we have defined

$$\delta_{ijkl} \equiv \delta_{ij}\delta_{kl} + \delta_{ik}\delta_{jl} + \delta_{il}\delta_{jk}, \tag{5}$$

$$\sigma_j^2 \equiv \int \mathrm{d}\boldsymbol{k}\, P_\phi(\boldsymbol{k})\, M^2(k)\, W^2(kR)\, (-k^2)^j, \tag{6}$$

where

$$M(k) \equiv \frac{3c^2}{5\Omega_m H_0^2}\, T(k) \tag{7}$$

and $T(k)$ is the CDM transfer function. (Strictly speaking, we are currently interested in the limit in which $W = 1$. We have defined the more general expression so that it can be used in the following subsections.) Thus,

$$\langle\Phi_{ij}\,\Phi_{kl}\rangle = \frac{\sigma_{NG}^2}{15}\delta_{ijkl}, \qquad \text{and} \tag{8}$$

$$\langle\Phi_{ij}\,\Phi_{kl}\,\Phi_{mn}\rangle = 2f_{nl}\frac{\gamma_{NG}^3}{135}\left[\delta_{ij}\delta_{klmn} + \delta_{kl}\delta_{ijmn} + \delta_{mn}\delta_{ijkl}\right] + \mathcal{O}(f_{nl}^3), \tag{9}$$

where

$$\frac{\sigma_{NG}^2}{15} = \frac{\sigma_2^2}{15} + 4f_{nl}^2\left[\left(\frac{\sigma_1^2}{3}\right)^2 + \frac{\sigma_0^2\sigma_2^2}{15}\right] \qquad \text{and} \qquad \frac{\gamma_{NG}^3}{135} = -2\frac{\sigma_1^2}{3}\frac{\sigma_2^2}{15}. \tag{10}$$

2.2 The smoothed initial field

In the spherical evolution model, the quantity of interest is the initial overdensity δ_l smoothed on some scale V. Most of the complication in f_{nl} models arises from the fact that the effect of smoothing is non-trivial. This nontriviality is a consequence of the fact that a smoothed Gaussian field is itself Gaussian, but this self-similarity does not hold for generic random fields.

We now calculate the distribution function of the initial overdensity δ_l smoothed on scale R in the f_{nl} model. Our goal is to approximate this initial PDF using the Edgeworth expansion:

$$p(\delta_l|R)\,\mathrm{d}\delta_l = \frac{e^{-\nu^2(R)/2}}{\sqrt{2\pi}}\left[1 + \frac{\sigma_{NG}(R)S_3(R)}{6}H_3(\nu(R))\right]\,\mathrm{d}\nu(R), \tag{11}$$

where $\nu(R) = \delta_l/\sigma_{NG}(R)$ and $H_3(\nu) = \nu(\nu^2 - 3)$. Therefore, we must specify how to calculate σ_{NG} and $\sigma_{NG}\,S_3$.

The Fourier transform of the initial overdensity is related to the Fourier transform of Φ by $\delta_k \equiv -k^2\, M(k)\, \Phi_k$. So spherical symmetry implies that the power spectrum and bispectrum of δ_l are

$$P_{\delta_l}(k) = (-k^2)^2 M^2(k) P_\Phi(k) = k^4 M^2(k) \left[P_\phi(k) + \frac{2 f_{nl}^2}{(2\pi)^3} \int \mathrm{d}\boldsymbol{q} P_\phi(q) P_\phi(|\boldsymbol{k}-\boldsymbol{q}|) \right], \tag{12}$$

$$B_{\delta_l}(k_1,k_2,k_{12}) = (-k_1^2)(-k_2^2)(-k_{12}^2) M(k_1) M(k_2) M(k_{12}) B_\Phi(k_1,k_2,k_{12}), \tag{13}$$

$$B_\Phi(k_1,k_2,k_{12}) \equiv 2 f_{nl}\ [P_\phi(k_1)P_\phi(k_2) + \text{cyclic}] + \mathcal{O}(f_{nl}^3). \tag{14}$$

From equations (8) and (9), we have

$$\sigma_{NG}^2 \equiv \langle \delta_l^2 \rangle = \frac{1}{(2\pi)^3} \int \frac{\mathrm{d}k}{k} 4\pi k^7 M^2(k) P_\Phi(k) W^2(kR), \tag{15}$$

$$\sigma_{NG} S_3 \equiv \frac{\langle \delta_l^3 \rangle}{\langle \delta_l^2 \rangle^{3/2}} = \frac{2 f_{nl} \gamma_{NG}^3 + \mathcal{O}(f_{nl}^3)}{\sigma_{NG}^3} \qquad \text{where} \tag{16}$$

$$2 f_{nl} \gamma_{NG}^3(R) = -\frac{2}{(2\pi)^4} \int \frac{\mathrm{d}k_1}{k_1} k_1^3 W(k_1 R) \int \frac{\mathrm{d}k_2}{k_2} k_2^3 W(k_2 R) \int \mathrm{d}\mu_{12}\, W(k_{12}R)\, B_{\delta_l}(k_1,k_2,k_{12}), \tag{17}$$

with $\mu_{12} \equiv \cos\theta_{12}$, and θ_{12} is the angle between $\boldsymbol{k}_1$ and $\boldsymbol{k}_2$: $k_{12}^2 \equiv k_1^2 + k_2^2 + 2k_1k_2\,\mu_{12}$.

To second order in f_{nl}, the variance $\sigma_{NG}^2(R)$ is the sum of two terms; one is the same as for the Gaussian, and the second, which is proportional to f_{nl}^2, involves a convolution of the power spectrum P_ϕ with itself. This term has two infra-red singularities (at $q=0$ and $\boldsymbol{k}=\boldsymbol{q}$ respectively) for $n_s < 4$. Fortunately, these can be removed by rewriting the power spectrum as

$$P_\Phi(k) = P_\phi(k) + \frac{2 f_{nl}^2}{(2\pi)^3} \int \mathrm{d}\,\boldsymbol{q}\, [P_\phi(q) P_\phi(|\boldsymbol{k}-\boldsymbol{q}|) - P_\phi(k) P_\phi(q) - P_\phi(k) P_\phi(|\boldsymbol{k}-\boldsymbol{q}|)], \tag{18}$$

where $P_\phi(k)$ has a new normalization (McDonald 2008). For $|f_{nl}| \le 100$, this renormalization is just a few percent effect, but the procedure is essential for removing the singularities.

Equation (17) indicates that $\langle \delta_l^3 \rangle$ scales linearly with f_{nl}. On scales larger than about $100h^{-1}$Mpc, the integral which defines γ_{NG}^3 can be approximated analytically (Scoccimarro et al. 2004), but on smaller scales, the integral must be evaluated numerically. For models of interest, σS_3 is only weakly scale dependent: e.g., it is $\approx -0.02(f_{nl}/100)$ on $\sim 100h^{-1}$Mpc, and is less than a factor of two larger on scales ($\sim 1h^{-1}$Mpc) (e.g., Figure 1 in Scoccimarro et al. 2004). This means that $|\sigma_{NG}\, S_3| \ll 1$ on the scales of interest in this paper, justifying our use of the Edgeworth expansion. In addition, note that if $\sigma_{NG}(R) S_3(R)$ were independent of R, then the Edgeworth expansion would be a function of ν only. In this case, the initial (non-Gaussian) PDF would be scale-independent, in the sense that the PDF would have the same functional form for all smoothing scales, just as it does for the Gaussian. Over a sufficiently narrow range of scales, this is a reasonable approximation.

2.3 The PDF of the smoothed, evolved, nonlinear overdensity

The previous section showed how to calculate the distribution of the initial overdensity δ_l. Nonlinear evolution changes this distributions; this section shows how to estimate the evolved, nonlinear PDF of the overdensity. As noted in the introduction, this can be done by following the same steps as in Lam & Sheth (2008), but with the non-Gaussian initial distributions. For brevity, we show results for the spherical evolution model only.

In the spherical model, the nonlinear overdensity in a region of volume V containing mass M is solely determined by the linear overdensity δ_l through a $1 \to 1$ mapping:

$$\rho \equiv 1 + \delta = \frac{M}{\bar\rho V} = \left(1 - \frac{\delta_l}{\delta_c}\right)^{-\delta_c}, \tag{19}$$

(Bernardeau 1994; Sheth 1998), where $\delta_c \approx 5/3$ and the exact value depends weakly on the cosmology. In this study we will use $\delta_c = 1.66$ which corresponds to the ΛCDM cosmology. The PDF of the nonlinear overdensity in a volume V associated with spherical collapse is

$$\rho^2 p(\rho|V) = p_{NG}\Big(\delta_l(\rho)|V_l(\rho)\Big)\, \nu\, \frac{\mathrm{d}\ln\nu}{\mathrm{d}\ln\rho}, \tag{20}$$

where $p_{NG}(\delta_l|V_l)$ is the initial PDF of δ_l at a given smoothing scale V_l. This with equation (11) implies that

$$\begin{aligned} \rho^2 p(\rho|V) &= \frac{1}{\sqrt{2\pi\sigma^2(\rho)}} \exp\left[-\frac{\delta_l^2(\rho)}{2\sigma^2(\rho)}\right] \left[1 - \frac{\delta_l(\rho)}{\delta_c} + \frac{\gamma_\sigma}{6}\delta_l(\rho)\right] \left[1 + \frac{\sigma(\rho) S_3(\rho)}{6}\, H_3\left(\frac{\delta_l(\rho)}{\sigma(\rho)}\right)\right], \\ &= \rho^2 p_{\rm G}(\rho|V)\ \left[1 + \frac{\sigma(\rho) S_3(\rho)}{6}\, H_3\left(\frac{\delta_l(\rho)}{\sigma(\rho)}\right)\right], \end{aligned} \tag{21}$$

where $p_{\rm G}$ denotes the smoothed nonlinear PDF assoociated with Gaussian initial conditions, $\sigma(\rho) = \sigma_{NG}(R = (3M/4\pi\bar\rho)^{1/3})$,

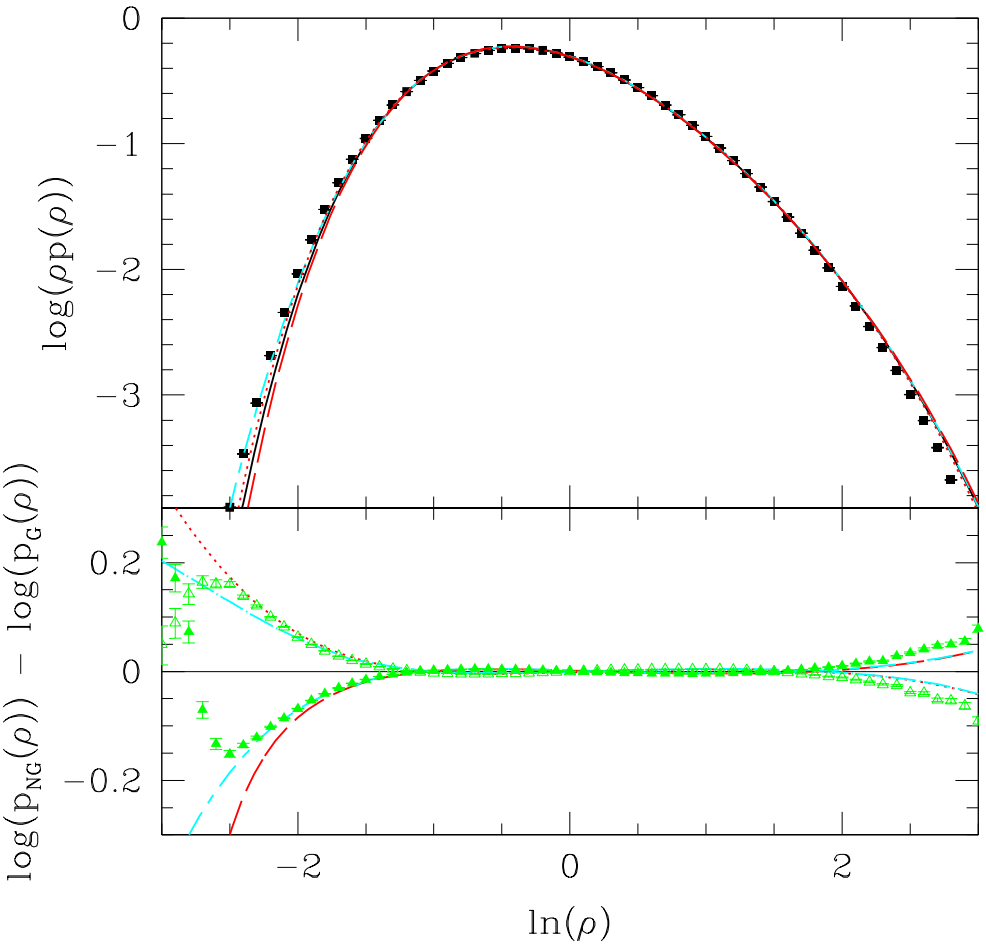

Figure 1. Nonlinear overdensity PDF using the spherical collapse model in cells of radius $8h^{-1}$Mpc. Long-dashed, solid, and dotted curves in the upper panel show $\ln(\rho\, p(\rho))$ (from equation 21) as a function of $\ln\rho$ for $f_{nl} = -100, 0$ and 100. Symbols show the PDF measured in the $f_{nl} = 100$ simulation, and long-dashed-short-dashed curve shows the associated Poisson-sampled prediction (equation 22). The lower panels show the log of the ratio between the $f_{nl} \neq 0$ predictions and that for Gaussian initial conditions, for which $f_{nl} = 0$. Filled and empty symbols are similar ratios of the measured PDFs for $f_{nl} = -100$ and 100 respectively.

and $\gamma_\sigma \equiv -3\,\mathrm{d}\ln\sigma^2/\mathrm{d}\ln M$ is not to be confused with the skewness parameter we defined earlier. Finally, we set $\rho' \equiv N\rho$ and $\rho'^2\, p'(\rho') \equiv \rho^2\, p(\rho)$ to ensure that $\int \mathrm{d}\rho'\, \rho'\, p'(\rho')$ and $\int \mathrm{d}\rho'\, p'(\rho')$ both equal unity (see discussion in Lam & Sheth 2008b,a).

The non-gaussian modification contributes the final term of the right hand side of equation (21). Since $\delta_l = 0$ when $\rho = 1$, there is little or no correction to the Gaussian case at $\rho \approx 1$. However, there is an effect at the low and high density tails. To see what it is, note that σS_3 is only a weak function of R, so it is a weak function of ρ, and hence the main ρ dependence is due to H_3. To see what this dependence is, suppose that $\gamma_\sigma = -6/5$ (this is close to its actual value on the scales we consider when comparing with simulations in the next section). Then $\delta_l/\sigma \approx (5/3)(1-\rho^{-3/5})/(\sigma_{\rm V}\rho^{-1/5}) \approx (5/3\sigma_{\rm V})(\rho^{1/5} - \rho^{-2/5})$, where $\sigma_{\rm V}$ is the variance of the initial field when $\rho = 1$. When $\rho \gg 1$, then $\delta_l/\sigma \approx (5/3\sigma_{\rm V})\,\rho^{1/5}$, so $H_3 \propto \rho^{3/5}$. As a result, for $f_{nl} > 0$, the high density tail of the PDF is increasing suppressed compared to the Gaussian case as ρ increases. At low densities, $\rho \ll 1$, then $\delta_l/\sigma \approx -(5/3\sigma_{\rm V})\,\rho^{-2/5}$, so $H_3 \propto -\rho^{-6/5}$: the low density tail is enhanced for $f_{nl} > 0$. The dependence on ρ is stronger for $\rho \ll 1$ than for $\rho \gg 1$, so we expect the underdense tail to be a good probe of f_{nl}. For sufficiently large $|\delta_l/\sigma|$, the non-Gaussian piece can be negative, signaling that our truncation of the Edgeworth expansion was inappropriate. Fortunately, we are generally only interested in scales that are not significantly affected by this truncation problem.

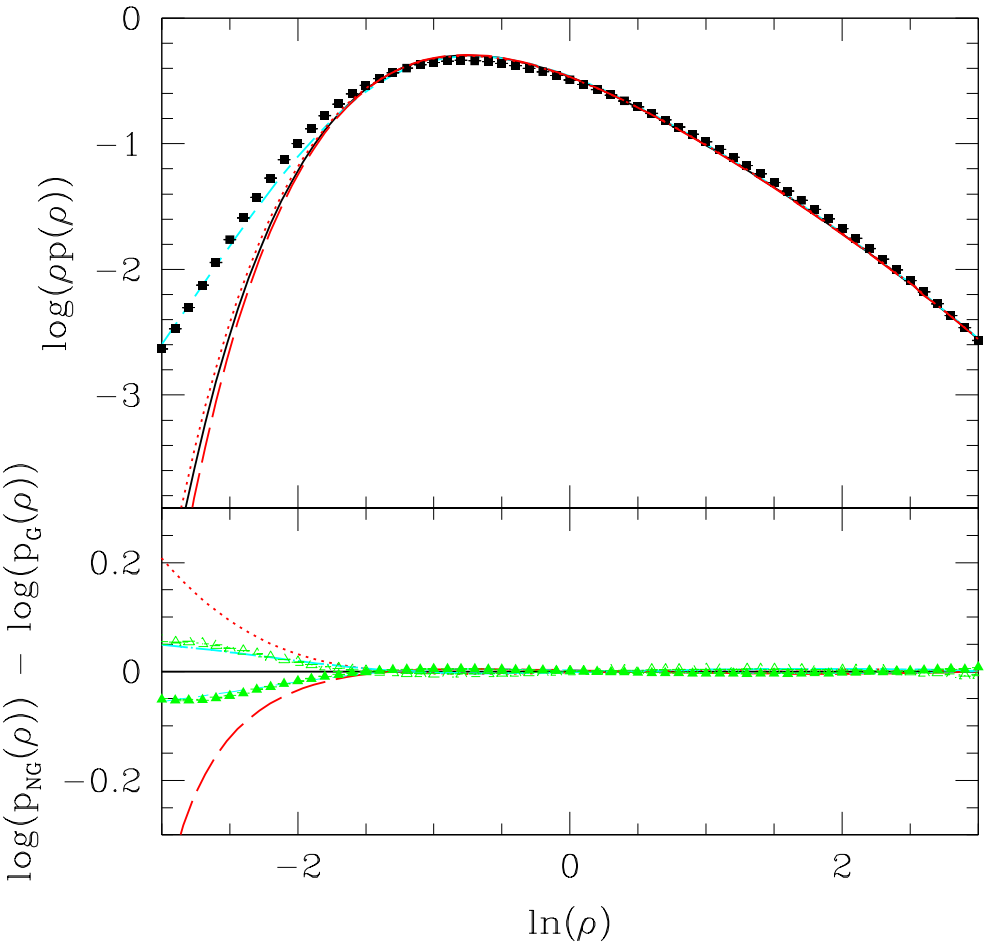

Figure 2. Same as previous figure, but for cells of radius $4h^{-1}$Mpc.

2.4 Comparison with simulations

We compare the predictions of our approach with measurements of the nonlinear PDF in numerical simulations from Desjacques et al. (2008). These followed the evolution of 1024^3 particles in a periodic cube of sides $1600\,h^{-1}$Mpc. The background cosmology is spatially flat, dominated by a cosmological constant, having $(\Omega_m, \Omega_b, n_s, h, \sigma_8) = (0.279, 0.0462, n_s = 0.96, 0.7, 0.81)$, so the particle mass was $3 \times 10^{11} h^{-1} M_\odot$. The simulations sample the density field using discrete particles. This produces discreteness effects which are largely irrelevant, except in the least dense tails of the PDF. (E.g., the average number of particles in spherical cells with radius $4h^{-1}$Mpc is ≈ 60. So discreteness effects are severe at $\rho < 1/6$.) We account for this using the Poisson model:

$$p(N|V) = \int dM\, p(M|V)\, p(N|M) \tag{22}$$

where $p(N|M,V) = (M/m_p)^N \exp(-M/m_p)/N!$, with m_p equal to the particle mass (Sheth 1996). We then set $\rho \equiv N/\bar{n}V$ when plotting the results.

The symbols in the top panel of Figure 1 show the measured PDF for counts in spheres of radius $8h^{-1}$Mpc for $f_{nl} = 100$. The dashed curve which is closest to these symbols shows equation (22) for $f_{nl} = 100$. The dashed, solid and dotted curves show the predictions of equation (21) for $f_{nl} = -100$, 0 and 100. The bottom panel shows the ratio of the counts in the f_{nl} models to those when $f_{nl} = 0$. The outer set of curves show equation (21) and the inner set show the effect of accounting for discreteness effects using equation (22). This shows that the PDF for positive f_{nl} is slightly skewed towards underdense regions, the reverse is true for negative f_{nl}, and our model provides an excellent description of these trends.

Figure 2 shows a similar analysis of the PDF on smaller scales, for which the discreteness effects are more pronounced:

at small ρ, the symbols in the top panel lie well above the curves associated with equation (21). However, our Poisson model for the discreteness effect appears to be rather good: the prediction associated with equation (22) provides a good description of the measurements. The bottom panel shows that discreteness effects tend to wash out the differences between the different f_{nl} runs, but that our Poisson model does an excellent job of accounting for this effect (the predictions at small ρ are almost indistinguishable from the measurements).

3 DISCUSSION

We used the spherical evolution model to study the nonlinear evolved probability distribution function of the dark matter density field in the local primordial non-Gaussian f_{nl} model. (The spherical model is able to provide a good description of the nonlinear PDF when $f_{nl} = 0$.) For currently acceptable values of f_{nl}, our approach shows that the signatures of primordial non-Gaussianity are small, but are most evident in underdense regions (equation 21 and related discussion). The PDF measured in simulations can be affected by discreteness effects, especially in small underdense cells. The effect of this can be approximated by using a Poisson counting model (equation 22). Once this is done, our model is in very good agreement with measurements in numerical simulations (Figures 1 and 2), so we hope our equation (21) will be useful in studies which require knowledge of the nonlinear evolved PDF.

Recently, following the same logic for why cluster abundances should be good probes of primordian non-Gaussianity, Kamionkowski et al. (2008) have suggested that void abundances should also be good probes. Our results provide further motivation for studying underdense regions. We are in the process of developing a more complete model of voids and void shapes (following Sheth & van de Weygaert 2004).

Finally, note that the parameter which describes the non-Gaussianity in the smoothed initial and final fields, $\sigma\, S_3$, is only weakly scale-dependent. Therefore, our analysis indicates that the non-gaussian distribution of the resulting nonlinear PDF (equation 21) can be written in terms of the scaled variable $\nu = \delta_l/\sigma$. So one could formulate a reconstruction of the initial f_{nl} field analogously to how this is done for the Gaussian case (Lam & Sheth 2008a). We have not pursued this further.

ACKNOWLEDGEMENTS

We thank V. Desjacques for help with measuring the PDFs in his simulations and R. Scoccimarro and E. Komatsu for many helpful discussions. Thanks also to S. Cole, K. Dolag, M. Grossi, W. Hu, Y. P. Jing, Z. Ma, T. Nishimichi, and R. Scoccimarro for discussions about resolution effects on the setting up of initial conditions in simulations.

REFERENCES

Afshordi N., Tolley A. J., 2008, ArXiv e-prints, astro-ph/0806.1046
Bernardeau F., 1994, Astron. Astrophys., 291, 697
Cole S., Kaiser N., 1989, Mon. Not. R. Astron. Soc., 237, 1127
Carbone C., Verde L., Matarrese S., 2008, Astrophys. J. Lett., 684, L1
Dalal N., Doré O., Huterer D., Shirokov A., 2008, Phys. Rev. D, 77, 123514
Desjacques V., Seljak U., Iliev I., 2008, Mon. Not. R. Astron. Soc., submitted (arXiv:0811.2748)
Grinstein B., Wise M., 1986, Astrophys. J., 310, 19
Grossi M., Branchini E., Dolag K., Matarrese S., Moscardini L., 2008, ArXiv e-prints, astro-ph/0805.0276
Hikage C., Matsubara T., Coles P., Liguori M., Hansen F. K., Matarrese S., 2008, Mon. Not. R. Astron. Soc., 389, 1439
Kaiser N., 1984, Astrophys. J. Lett., 284, L9
Kamionkowski M., Verde L., Jimenez R., 2008, ArXiv e-prints, astro-ph/0809.0506
Komatsu E., Dunkley J., Nolta M. R., Bennett C. L., Gold B., Hinshaw G., Jarosik N., Larson D., Limon M., Page L., Spergel D. N., Halpern M., Hill R. S., Kogut A., Meyer S. S., Tucker G. S., Weiland J. L., Wollack E., Wright E. L., 2008, ArXiv e-prints, astro-ph/0803.0547
Lam T. Y., Sheth R. K., 2008a, Mon. Not. R. Astron. Soc., 386, 407
Lam T. Y., Sheth R. K., 2008b, Mon. Not. R. Astron. Soc., 389, 1249
Lo Verde M., Miller A., Shandera S., Verde L., 2008, Journal of Cosmology and Astro-Particle Physics, 4, 14
Lucchin F., Matarrese S., Vittorio N., 1988, Astrophys. J. Lett., 330, L21
Matarrese S., Verde L., 2008, Astrophys. J. Lett., 677, L77
Matarrese S., Verde L., Jimenez R., 2000, Astrophys. J., 541, 10
McDonald P., 2008, ArXiv e-prints, astro-ph/0806.1061
McEwen J. D., Hobson M. P., Lasenby A. N., Mortlock D. J., 2008, Mon. Not. R. Astron. Soc., 388, 659

Mo H. J., White S. D. M., 1996, Mon. Not. R. Astron. Soc., 282, 347
Robinson J., Baker J., 2000, Mon. Not. R. Astron. Soc., 311, 781
Scoccimarro R., Sefusatti E., Zaldarriaga M., 2004, Phys. Rev. D, 69, 103513
Sefusatti E., Komatsu E., 2007, Phys. Rev. D, 76, 083004
Sheth R. K., 1996, Mon. Not. R. Astron. Soc., 279, 1310
Sheth R. K., 1998, Mon. Not. R. Astron. Soc., 300, 1057
Sheth R. K., Tormen G., 1999, Mon. Not. R. Astron. Soc., 308, 119
Sheth R. K., van de Weygaert R., 2004, Mon. Not. R. Astron. Soc., 350, 517
Slosar A., 2008, ArXiv e-prints, astro-ph/0808.0044
Slosar A., Hirata C., Seljak U., Ho S., Padmanabhan N., 2008, Journal of Cosmology and Astro-Particle Physics, 8, 31
Taruya A., Koyama K., Matsubara T., 2008, ArXiv e-prints, astro-ph/0808.4085
Yadav A. P. S., Wandelt B. D., 2008, Physical Review Letters, 100, 181301